Journal of Chemical Engineering & Process Technology

Sashi Kumar et al., J Chem Eng Process Technol 2011, S1
DOI: 10.4172/2157-7048.S1-002

Research Article Open Access

Understanding the Compatibility of Thermal Mass Flow Meter with Various Process Gases

Sashi Kumar GN*, Mahendra AK and Gouthaman G

Machine Dynamics Division, Chemical Technology Group, Bhabha Atomic Research Centre, Mumbai, India

Abstract

A majority of vacuum processes use the Thermal Mass Flow Meter (TMFM) as metering device for process gas. The purpose of this paper is to establish cross compatibility relationship of the TMFM with different process gases. This paper uses a compressible Computational Fluid Dynamic (CFD) solver to understand the behavior of TMFM with different process gases. The change in the characteristic curve at lower pressures has also been studied. Empirical correlations have been developed so that the change in characteristic curve of TMFM can be predicted accurately for different gases based on their physical properties.

Keywords: Thermal Mass Flow Meter; Computational Fluid Dynamics; Characteristic curve; Process gas; Open FOAM; Empirical correlation

Nomenclature: C_p: Specific heat at constant pressure, J/kg K; k: Thermal conductivity of gas, W/m k; L: Length of capillary; L_s: Distance from center of TMFM to the temperature senor, m; M: Molecular weight, kg/kg mole; $\dot{m}$: Mass flow rate of gas, kg/s; N_{Gz}: Graetz number; N_{Kn}: Knudsen number; N_{Pr}: Prandtl number; N_{Re}: Reynolds number; p: Pressure, N/m^2; t: Time, sec; T: Temperature, K; T_w: Temperature of wall at the heater, K; T_f: Temperature of gas, K; q_c: Heat flux from heater, W/m^2; $\dot{V}$: Molar flow rate of gas, SCCM; α, β, $F_{1,2}$, f: Constants; ρ: Density of gas, kg/m^3; γ: Gamma, ratio of specific heats; μ: Viscosity, kg/m

Introduction

Devices to measure flow accurately have gained importance in many chemical process industry applications. The precise control of flow in the process warrants minimal error in the measuring instruments. Improved performance, low cost, low-pressure drop, compactness in size and a small response time have helped thermal mass flow meter (TMFM) gain acceptance in the industry for gas flow measurements [1-3]. Thermal mass flow meters are widely used in measuring gas flows with applications to semiconductor manufacturing gas distribution, heating, ventilation, air-conditioning, human inhalation system, environmental safety, etc.

This device is called 'immiscible' (or 'insertion' meters) when it is immersed in the fluid stream. They typically measure gas velocity over the range of 0.5 to 150nm/s [4]. A second common type called 'in-line' meter has dual-sensors permanently fitted into a pipe or tube (8 to 300mm in dia), which are directly calibrated for the total gas mass flow rate flowing though the pipe. The third type is a 'capillary-tube' meter, which is installed as in-line mass flow meter for low gas flows. This type has further sub-classification as 'constant temperature' and 'constant heat flux' based thermal mass flow meters. In 'constant temperature' thermal mass flow meter a constant temperature difference (T_w-T_f) is maintained and the amount of heat flux (q_c) imparted by the heater to fluid is measured. T_w is temperature of wall at the heater and T_f is the gas temperature. Since the gas molecules carry the heat away from the heated sensor, the heat flux q_c is a direct measure of the gas mass flow rate.

In this paper the 'constant heat flux' based 'capillary-tube' type thermal mass flow meter has been studied in detail. Figure 1a shows the typical construction of the thermal mass flow meter. The capillary tube has electronics mounted on it that can heat the capillary. A constant heat flux q_c is always supplied through this heater. Two temperature sensors (thermocouples) are mounted on the wall of the capillary. They are generally equidistant from the heater (center of heater is taken as origin of axis). Figure 1a shows two temperature sensors at positions L_s and -L_s from the heater. The solid line in Figure1b is typical temperature along the wall of the capillary when gas flow rate is zero. When the gas starts flowing the molecules of gas carry the heat away from the heater along the flow direction. This induces skewness in the temperatures along the wall of the capillary. It is illustrated by dotted line in Figure 1b. This skewness increases with increase in mass flow rate. The temperature difference between the two temperature sensors (ΔT) is a measure of the skewness. Figure 1c shows a typical characteristic curve 'ΔT versus mass flow rate' for a particular gas. The sensitivity of this instrument is proportional to the slope of this curve (ΔT/mass flow rate). A high sensitivity/slope is desirable for better accuracy. So a positive and high slope is generally the aim when designing a mass flow meter. ΔT is found to be linearly proportional to small gas mass flow rates. Represented by line OA in Figure 1c called as 'linear zone'. As one keeps on increasing the flow rate above point A the ΔT is non-linearly proportional to the gas mass flow rate.

Represented by line AC in Figure 1c called as 'non-linear zone'. There is always a positive ΔT with increase in mass flow rate for the region OC, i.e. a positive slope remains within this zone. Slope of the ΔT reaches its maximum at point C and a further increase in mass flow rate decrease the ΔT. This behavior, which is common for all gases, is a function of specific heat of the gas. More elaboration can be found in section 3 of this paper. It is worth noting in Figure 1c the slope of curve CD is negative. This is non-operable zone of the mass flow meter.

***Corresponding author:** Sashi Kumar GN, Machine Dynamics Division, Chemical Technology Group, Bhabha Atomic Research Centre, Mumbai, India, E-mail: gnsk@barc.gov.in

Received September 23, 2011; **Accepted** January 03, 2012; **Published** January 23, 2012

Citation: Sashi Kumar GN, Mahendra AK, Gouthaman G (2012) Understanding the Compatibility of Thermal Mass Flow Meter with Various Process Gases. J Chem Eng Process Technol S1:002. doi:10.4172/2157-7048.S1-002

Although the slope is positive till the point C, the curve becomes more flat above point B reducing the sensitivity of the instrument. A point B is chosen by the designer below the point C so that the slope/sensitivity of the instrument is within the required specification. Zone OB is the 'operating zone' of the instrument. The mass flow rate at which ΔT becomes negligible can be termed as point of inflection (point C in Figure 1c) after which the TMFM predicts wrong results.

The instrument needs to be calibrated exhaustively with primary standard like gravimetry, etc. if the 'operating zone' extends to the 'non-linear zone'. In contrast one requires the value of sensitivity/slope if the 'operating zone' is within the 'linear zone' of the characteristic curve.

The electronics designed along with TMFM are based on measurement of constant temperature difference. This calls for curtailing the operating zone to the linear zone (Figure 1c). Komiya et al. [5] has derived an analytical expression for the ΔT as function parameters such as dimension of TMFM, heat supplied and properties of gas based on a simple flow model. Various gases were analyzed and a relation was obtained which makes ΔT reproducesable uniquely for all gases when mass flow rate was weighed with specific heat x density.

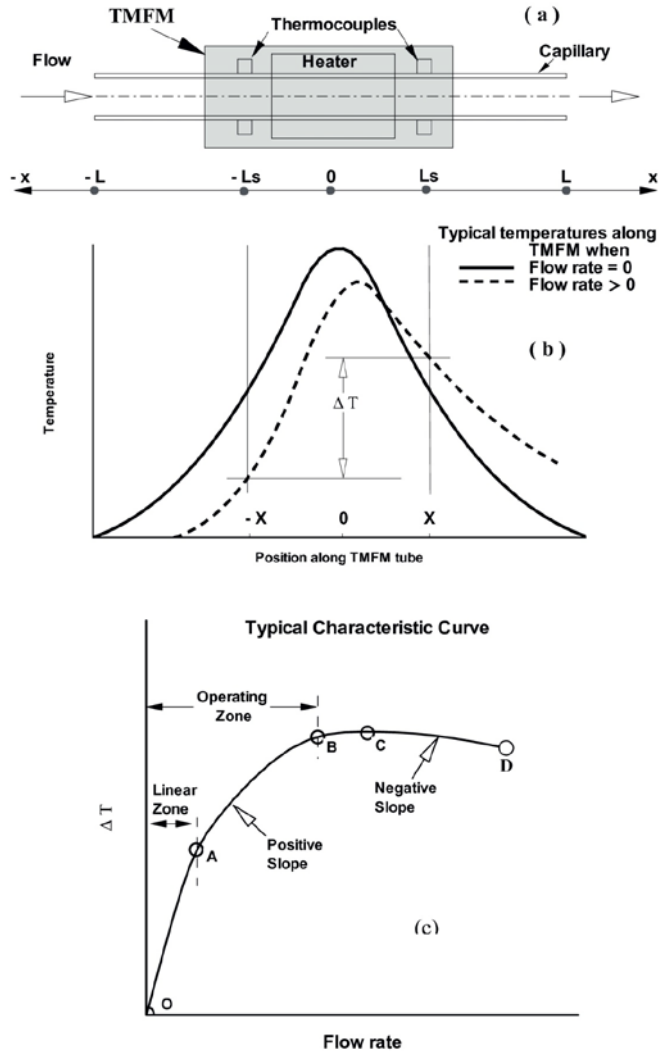

Figure 1: TMFM schematic, principle and zones of operation.

This correlation emphasizes the role of pressure ($p = \rho \frac{R}{M} T$) in the operation of TMFM. Kim et al. [6] has obtained a correlation that can predict the linear range of the TMFM and predicts the inflection point. Later Kim et al. [7] has extended on similar lines to predict the sensitivity (i.e. $\left.\frac{\Delta T}{\dot{m}}\right|_{\dot{m}=0}$) of TMFM. These correlations show that sensitivity depends on specific heat of the gas when a given TMFM, is operated with different gases.

Most designers calibrate the TMFM for nitrogen gas. The sensitivity of the instrument changes with process gas (such as CO_2, Argon, etc.). In this paper the characteristic curves for different gases have been compared and a correlation has been developed so that any process gas characteristic curve can be obtained. The change in characteristic curve of TMFM with operating pressure of the instrument has been studied. The questions raised in the literature have been addressed.

The details of the computational fluid dynamics solver used for this problem and validation test case with nitrogen gas are elaborated in section 2. Section 3 compares the characteristic curves for different gases studied with CFD solver. Section 4 discusses the cases elaborated in section 3 for lower pressures. Conclusions are given in section 5.

Details of CFD and its Validation

The continuity equation, momentum and energy equations are solved simultaneously along with equation of state. The 3-D compressible Navier-Stokes equation can be represented in conservative form as

$$\frac{\partial U}{\partial t} + \frac{\partial}{\partial x}(GX) + \frac{\partial}{\partial y}(GY) + \frac{\partial}{\partial z}(GZ) = 0 \qquad (1)$$

where the state vector U and the flux vectors GX, GY and GZ are defined as:

$$U = \begin{pmatrix} \rho \\ \rho u \\ \rho v \\ \rho w \\ \rho E \end{pmatrix}; GX = \begin{pmatrix} \rho u \\ \rho u^2 + p - \tau_{xx} \\ \rho uv - \tau_{xy} \\ \rho uw - \tau_{xz} \\ \rho uE + up - v\tau_{xx} - v\tau_{xy} - w\tau_{xz} + q_x \end{pmatrix};$$

$$GY = \begin{pmatrix} \rho v \\ \rho uv - \tau_{yx} \\ \rho v^2 + p - \tau_{yy} \\ \rho vw - \tau_{yz} \\ \rho vE + vp - u\tau_{yx} - v\tau_{yy} - w\tau_{yz} + q_y \end{pmatrix}; \qquad (2)$$

$$GZ = \begin{pmatrix} \rho w \\ \rho uw - \tau_{zx} \\ \rho vw - \tau_{zy} \\ \rho w^2 + p - \tau_{zz} \\ \rho wE + wp - u\tau_{zx} - v\tau_{zy} - w\tau_{zz} + q_z \end{pmatrix}$$

$$p = \rho \frac{R}{M} T \qquad (3)$$

$$C_p - C_v = \frac{R}{M} \quad (4)$$

Where u, v and w are the velocity components in cartesan frame, ρ is the density, E is the total energy, T is the static temperature, τ is the shear stress tensor, q is the heat flux vector and p is the pressure which is calculated from equation of state of perfect gas. Eq. (4) holds for a thermally perfect gas, but C_p is assumed to be constant. The above equations were solved with axi-symmetric or wedge approximation. This reduces the computational load required for the problem. Since TMFM is axi-symmetric in nature, a wedge as shown in Figure 2a is sufficient to represent the whole geometry.

The density based compressible finite volume flow solver 'rhoPimpleFoam' has been used for solving the problem. RhoPimpleFoam used in this paper, is the version available in 'Open FOAM 1.7.1' software [8]. Open FOAM 1.7.1 is an open-source CFD platform that contains numerous validated solvers. RhoPimpleFoam is a transient flow solver that can operate in laminar/turbulent flow in high vacuum applications [8]. The Pimple algorithm has better stability when using larger time steps. All the cases solved in this paper are with

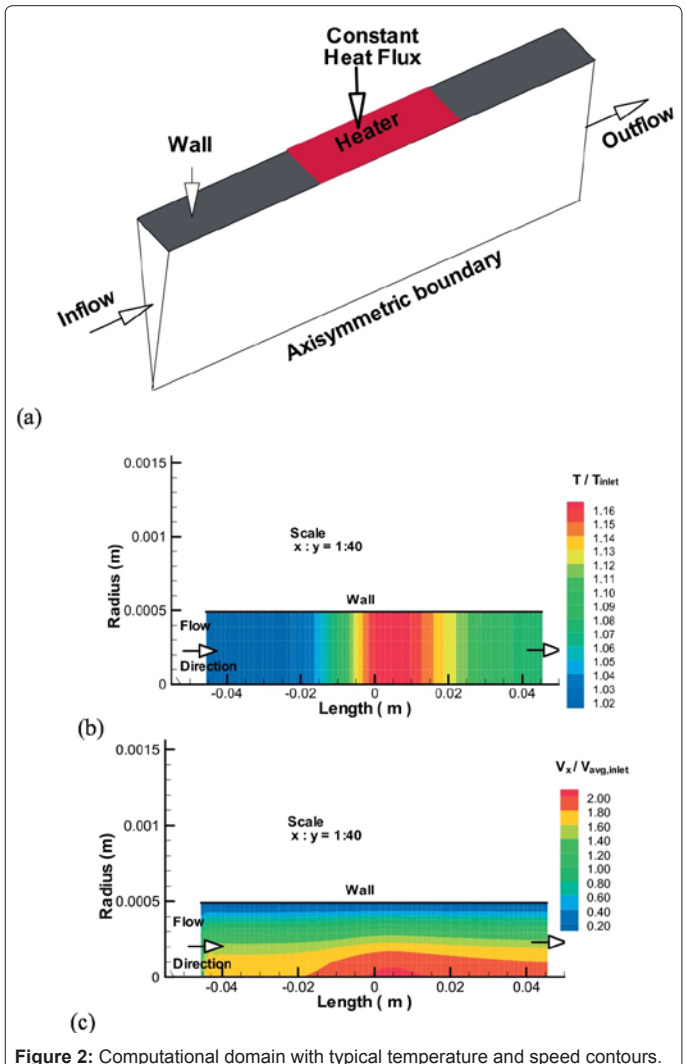

Figure 2: Computational domain with typical temperature and speed contours.

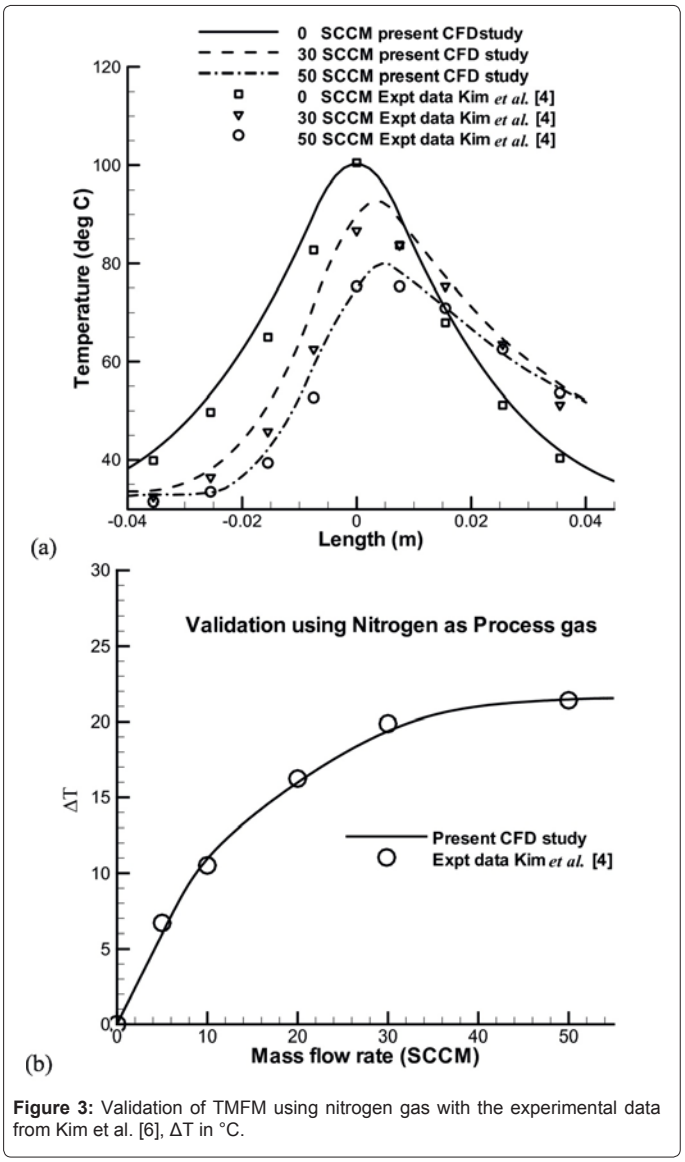

Figure 3: Validation of TMFM using nitrogen gas with the experimental data from Kim et al. [6], ΔT in °C.

N_{Re} < 10. The laminar solver was invoked with pseudo-transient to achieve the steady state solution of the TMFM's.

Studied with 3 grid sizes (70x7) Coarse (150x15) Medium and (300x 30) fine. Grid was generated using block Mesh utility of Open FOAM. Five-order drop in residue for energy equation was chosen as the convergence criteria. The ΔT (as defined in Figure1b) was determined at zero flow conditions with coarse, medium and fine grids and their values are 2.1C, 0.3C and 0.1C for respectively. In this paper the computational results discussed are with the medium grid of 150 x15 nodes.

Validation test case

The TMFM design discussed in reference [6] by Kim et al. has been used as the validation test case. The analysis is done on the capillary tube of 91mm length has inner diameter 0.977mm. The heater consists of 14.8mm wide, is centrally located on this capillary tube. L_s is chosen as 7.5mm (described in Figure 1a). Figure 2a gives illustration of boundary conditions used in the flow domain. Figure 2b and 2c shows

the temperature and speed contours (normalized by inlet values) obtained from CFD for a typical validation flow rate. Although Figure 2c shows a disturbed velocity profile at the center of the axis, yet there is no onset of turbulence.

The Figure 3a and 3b compares the results for various flow rates with the experimental values. The CFD results are found to be comparable with experimental data. The higher values of temperatures seen in Figure 3a can be attributed to two factors. First the metallic wall is not considered for simulation. A metallic wall will drop the temperature on the surface by a few degrees. Secondly the experiment was conducted in vacuum chamber hence adiabatic boundary condition was used. There could be a little convection heat loss, which was not simulated. Figure 3b shows a good agreement with the experimental values. This shows that neglecting wall in the simulation is of minimal consequence when ΔT is the measured.

Change in Process Gas and its Effects on Sensitivity

TMFM is sensitive to change in process gas, which is metered. Literature speaks of the dependability on the specific heat and density of the gas in evaluating the scaling parameter [5]. Here a few cases are considered to illustrate the phenomenon and prove/disprove the earlier claims made by researchers. Consider the TMFM designed for nitrogen as process gas, the one used for validation in previous section.

TMFM was simulated with Argon gas, CO_2 gas and butane gas for different flow rates, the value of ΔT is recorded. Table 1 gives the properties of the process gases studied. The properties are recorded

Process Gas	C_P (J/kg.K)	μ x 10^6 (kg/ m.s)	k (W/m.K)	N_{Pr}
Argon	516	22.9	0.0177	0.668
Nitrogen	1031	18.0	0.026	0.714
Carbon dioxide	861	15.0	0.0166	0.778
Butane	1695	7.6	0.016	0.805

Table 1: Properties of various process gases studied (at 303 K) [10].

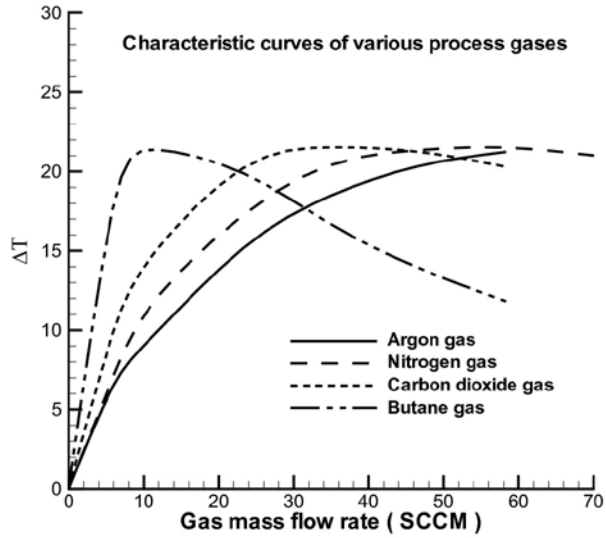

Figure 4: ΔT (°C) versus mass flow rate for different gases.

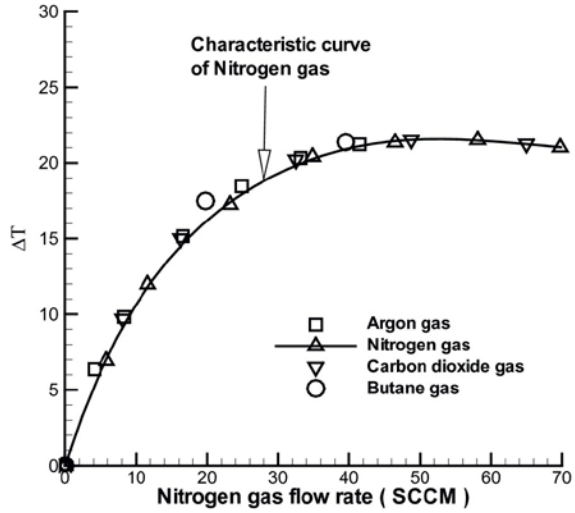

Figure 5: ΔT (°C) versus scaled mass flow rate using Equation 11 (gas 2 is Nitrogen).

at the inlet temperature (303K). Figure 4 shows the results obtained from the simulation studies with these gases. The job at hand is to find a suitable scaling parameter such that all the four different curves (characteristic curves of the gases studied) in Figure 4 merge into a single curve. This single curve will be the characteristic curve of reference gas that is generally, provided by the supplier of the instrument. The terminology is as follows: New process gas is "Gas 1" and the Reference gas is 'Gas 2' and the scaling factor is $F_{1,2}$. Nitrogen gas has been chosen as 'Gas 2' in this paper. On obtaining the value of $F_{1,2}$ for a new gas, the characteristic curve can be generated from the characteristic curve of the reference gas.

The heat transfer characteristic of the fluid depends on the Reynolds number (N_{Re}) at which it is being operated, Prandtl number (N_{Pr}) of the fluid. For this case of capillary flow with constant heat flux and N_{Re} < 10, the Nusselt number (N_{Nu}) would remain a constant (= 48/11) [9]. The dependability on Graetz number (N_{Gr}= N_{Re}xN_{Pr}) is negligible for such capillary flows (in TMFM).

The mass flow rate in TMFM is directly proportional to the ΔT produced. Also for a given mass flow meter the maximum ΔT the instrument can produce is independent on the properties of the process gas. Hence in order to study the scalability of TMFM with different gases, it is sufficient to scale the molar flow rate $\dot{V}$ (in SCCM) for fixed ΔT. The target of this work is to develop a scaling factor ($F_{1,2}$) for various process gases.

$$\text{Thus } \left.\frac{\Delta T}{\dot{V}}\right|_{Gas1} = F_{2,1} \times \left.\frac{\Delta T}{\dot{V}}\right|_{Gas2} \tag{5}$$

At constant ΔT Equation 7 becomes

$$\left.\dot{V}\right|_{Gas1} = F_{1,2} \times \left.\dot{V}\right|_{Gas2} \tag{6}$$

By method of dimensionless analysis the expression for $F_{1,2}$ is obtained.

The variables in this problem are

1. Mass flow rate in SCCM $\dot{V}$
2. Specific heat C_p
3. Temperature difference ΔT
4. Heat flux supplied to TMFM $\dot{q}$
5. Molecular weight M
6. Surface area of heater A

$$\dot{V} \propto C_p^{\alpha} \times \Delta T^{\beta} \times \dot{q}^{\delta} \times M^{\chi} \times A^{\eta} \tag{7}$$

$$(Mole.T^{-1}) = (L^2.T^{-2}.\Theta)^{\alpha} \times (\Theta)^{\beta} \times (M.T^{-3})\delta \times (M.Mole^{-1})^{\chi} \times (L^2)^{\eta} \tag{8}$$

Solving Equation (8) using dimensionless analysis yields

$\alpha = -1, \beta = 1, \Delta = 1, \chi = -1, \eta = 1$

Equation 7 becomes

$$\dot{V} \propto \frac{\Delta T, \dot{q}, A}{C_p.M} \tag{9}$$

Present analysis is for change in process gas in a given TMFM. So, the heater surface area and heat flux of the heater in the TMFM will remain as constant. Scaling is required at constant ΔT, so Equation (9) reduces to

$$\dot{V} \propto \left.\frac{1}{C_p.M}\right|_{\Delta T, \dot{q}, A} \tag{10}$$

When comparing the performance of two gases in a given TMFM Equation 10 becomes

$$\frac{\dot{V}_1}{\dot{V}_2} = \frac{(C_p.M)|_2}{(C_p.M)|_1} \tag{11}$$

Equation 11 needs to be checked with various process gases. The nitrogen gas characteristic curve (as shown Figure 5) should be reproduced from characteristic curve of any other gas after scaling. In order to quantify the error introduced by Eq. 11, an L_2 norm of the relative error is defined by following equation.

Gas 1	$F_{1,2}$ (Equation 11)	Error $\|\|E\|\|_2$ (of Equation 11)	$\gamma = \frac{C_p}{C_v}$
Ammonia	0.7917	+4.8815	1.2951
Argon	1.4007	-0.0878	1.6752
Butane	0.2933	-0.2726	1.0921
CO_2	0.7624	+6.5351	1.2811
Ethane	0.5359	-2.3810	1.1823
Helium	1.4178	+1.1349	1.6892
Hydrogen	0.9981	-1.1563	1.4029
Methane	0.7956	+8.2104	1.2969
Nitrogen	0.9999	-0.0003	1.4040

*Gas 2 is chosen as Nitrogen

Table 2: The values of $^*F_{1,2}$ for the process gases considered.

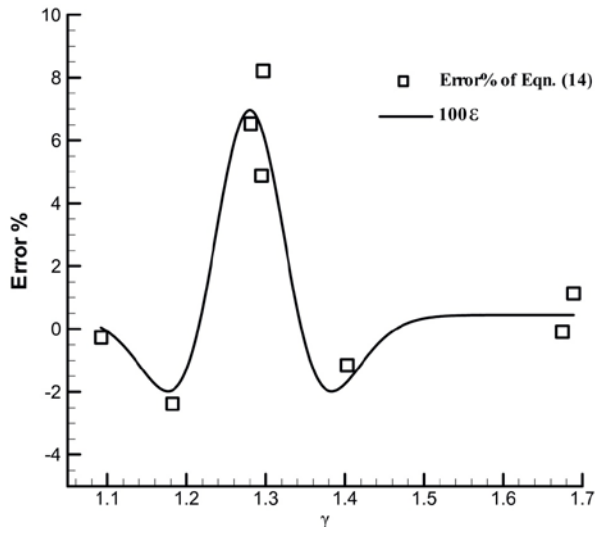

Figure 6: The regression analysis to evaluate the Gaussian radial basis function.

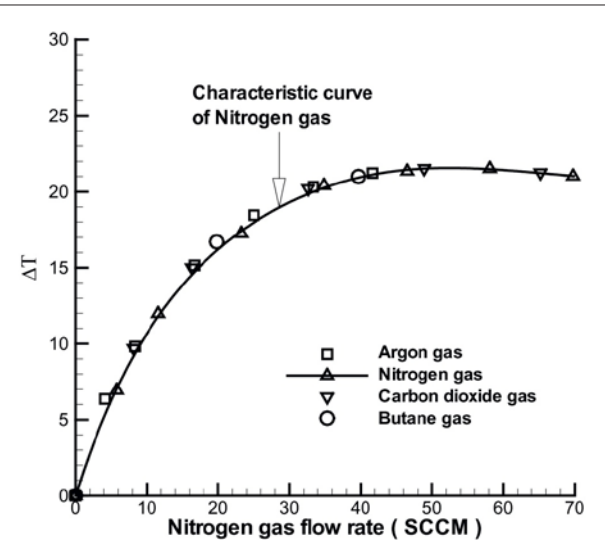

Figure 7: ΔT (°C) versus scaled mass flow rate using Eqation 15 (gas 2 is Nitrogen).

$$\|Error\|_2 = \sqrt{\frac{\sum_{i \in N} \left(\frac{y_{S,i} - y_{T,i}}{y_{T,i}} \right)^2}{N}} \tag{12}$$

where $y_{S,i}$ and $y_{T,i}$ are scaled value of ΔT and corresponding value of ΔT for nitrogen gas for a given molar flow.

Apart from the four gases mentioned earlier the analysis was done on five more gases to check the validity of Equation 11. The results are tabulated in Table 2.

It is observed that although Equation 11 predicts many of gas characteristics accurately, yet there is a considerable deviation for some of them. Such an error is unacceptable for an instrument like TMFM. A correction for Equation 11 is proposed to minimize the error.

$$\frac{\dot{V}_1}{\dot{V}_2} = \frac{(C_p.M)\big|_2}{(C_p.M)\big|_1} \times f \text{ Where the correction factor } f = \frac{1}{(1+\varepsilon)} \quad (13)$$

ε is a parameter modeled as a modified Gaussian radial basis function with γ as independent variable. The use of γ as a variable accounts for the compressibility effects of the gas, if any. The form of equation proposed is as follows.

$$100\varepsilon = A + B(e^{-cr^2}) + D(e^{-cr^2})^2 \text{ where } r = (\gamma\text{-}1.28) \quad (14)$$

A regression analysis with the data from Table 2 yields

A = 0.44623; B = -14.187; C = +100; D = +20.706

The comparison between the data and Equation (14) is shown in Figure 6.

Equation 13 was able to retain the error within 2% for all the cases considered for analysis (Figure 7). Table 3 gives a quantitative comparison of Equation 11 and Equation 13.

Operation at Low Pressure

Gas 1	$F_{1,2}$ (Eq. 11)	Error $\|\|E\|\|_2$ (of Eq. 11)	$F_{1,2}$ (Eq. 13)	% Error $\|\|E\|\|_2$ (of Eq. 13)
Ammonia	0.7917	+4.8815	0.7443	-1.3939
Argon	1.4007	-0.0878	1.3945	-0.5317
Butane	0.2933	-0.2726	0.2931	-0.3196
CO_2	0.7624	+6.5351	0.7128	-0.3992
Ethane	0.5359	-2.3810	0.5465	-0.4437
Helium	1.4178	+1.1349	1.4115	+0.6856
Hydrogen	0.9981	-1.1563	1.0151	+0.5271
Methane	0.7956	+8.2104	0.7491	+1.8837
Nitrogen	0.9999	-0.0003	1	0

*Gas 2 is chosen as Nitrogen

Table 3: The values of $^*F_{1,2}$ for the process gases considered.

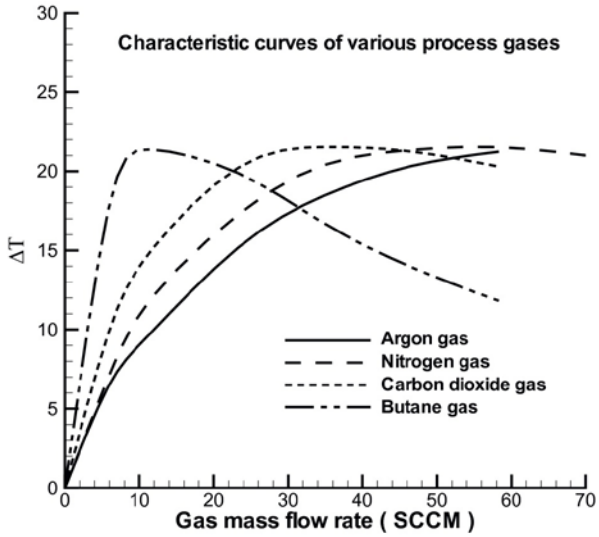

Figure 8: ΔT (°C) versus mass flow rate of different gases at low pressure.

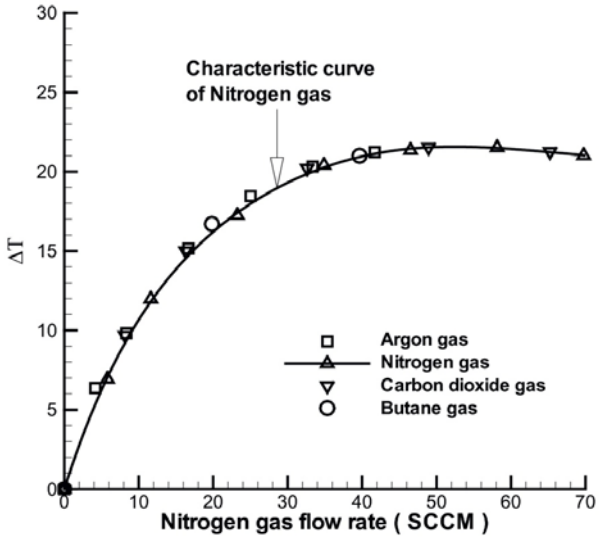

Figure 9: ΔT (°C) versus scaled mass flow rate using Equation 13 (gas 2 is Nitrogen) at low pressure.

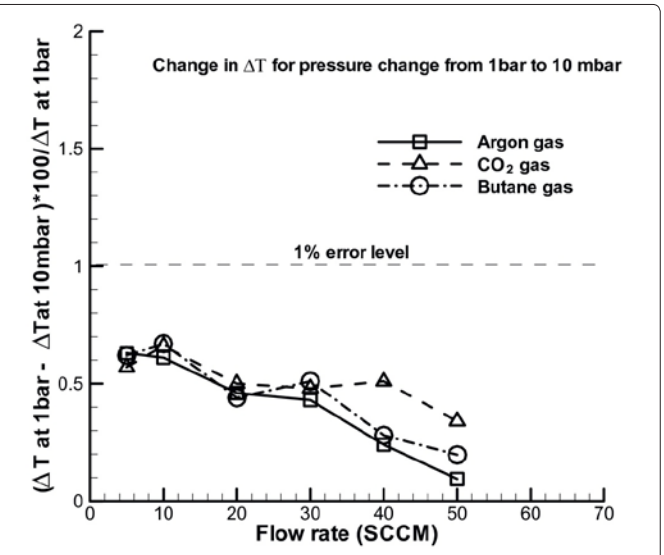

Figure 10: Percentage relative change in ΔT with change in pressure.

The Navier-Stokes solver with no slip walls has been used for all problems in this paper. This solver does not contain slip flow model/ boundary conditions and an attempt is made to solve TMFM problem in continuum regime. The cases discussed in section (3) have been repeated with a lower pressure of 10^3 Pa. Figure 8 and 9 (at a pressure of 10^3 Pa) shows that there is minimal effect of pressure on the mass flow meter. Figure 10 show that the change in ΔT < 1% for a corresponding drop in pressure from 1bar to 10 mbar. For all practical purposes the effect of pressure on TMFM (provided N_{Kn} < 0.1) can be neglected. The expressions derived in section 3 will be independent of operating pressure of the instrument. Investigations are needed for slip flow (0.1 > N_{Kn} > 1) and free molecular flow regimes (N_{Kn} > 10) to establish the effect of pressure.

Conclusion

The thermal mass flow meter has been simulated with compressible finite volume solver and validated. The characteristic curve for various process gases has been studied. An empirical correlation was developed which predicts the change in sensitivity with various process gases with good accuracy for a given TMFM.

References

1. Hardy JE, Hylton JO, McKnight TE, Remenyik CJ, Ruppel FR (1999) Flow Measurement Methods and Applications. John Wiley & Sons Inc. New York, USA.
2. Hinkle LD, Mariano CF (1991) Toward understanding the fundamental mechanisms and properties of the thermal mass flow controller. J Vac Sci Technol 9: 2043-2047.
3. Tison SA (1996) A critical evaluation of thermal mass flow meters. J Vac Sci Technol 14: 2582-2591.
4. Olin JG (1999) Industrial thermal mass flow meters.
5. Komiya K, Higuchi F, Ohtani K (1998) Characteristics of a thermal gas flowmeter. Rev Sci Instrum 59: 477-479.
6. Kim DK, Han Y II, Kim SJ (2007) Study on the steady-state characteristics of the sensor tube of a thermal mass flow meter. I J Heat Mass Transfer 50: 1206-1211.
7. Kim TH, Kim DK, Kim SJ (2009) Study of the sensitivity of a thermal flow sensor. I J Heat Mass Transfer 52: 2140-2144.
8. http://www.openfoam.com
9. Incropera FP, DeWitt DP, Bergman TL, Lavine AS (2002) Fundamentals of Heat and Mass Transfer. (5th edn), John Wiley & Sons Inc. New York, USA.
10. Perry RH, Green DW (1997) Perry's Chemical Engineers' Handbook. (7th edn), McGraw-Hill, USA.